IEEE Access
Multidisciplinary | Rapid Review | Open Access Journal

Received 11 January 2023, accepted 4 February 2023, date of publication 9 February 2023, date of current version 23 March 2023.

Digital Object Identifier 10.1109/ACCESS.2023.3243620

RESEARCH ARTICLE

Learning Car-Following Behaviors for a Connected Automated Vehicle System: An Improved Sequence-to-Sequence Deep Learning Model

WENQI LU[1], ZIWEI YI[1], BINGJIE LIANG[2], YIKANG RUI[1], AND BIN RAN[1]
[1]School of Transportation, Southeast University, Nanjing, Jiangsu 211189, China
[2]School of Traffic and Transportation, Beijing Jiaotong University, Beijing 100044, China

Corresponding author: Yikang Rui (101012189@seu.edu.cn)

This work was supported in part by Key Research and Development Program of Shandong Province, China, under Grant 2020CXGC010118, in part by the Natural Science Foundation of Beijing under Grant 9212014, in part by the National Natural Science Foundation of China under Grant 41971342, and in part by the Scientific Research Foundation of Graduate School of Southeast University under Grant YBPY2161.

ABSTRACT Data-driven car-following modeling is of great significance to traffic behavior analysis and the development of connected automated vehicle (CAV) technology. The existing researches focus on reproducing the car-following process by capturing the behavior of the host vehicle using the information of its nearest preceding vehicle. While the other preceding vehicles may affect the host vehicle as well. To fill the gap above, this paper presents an improved sequence-to-sequence deep learning-based (ISDL) car-following model for a CAV system. Firstly, the kinematics information considering the multiple preceding vehicles are organized as the input characteristics. Secondly, an improved sequence-to-sequence deep learning framework is proposed by integrating an encoder with the bidirectional gated recurrent unit (GRU) neural network and a decoder using an attention-based GRU neural network in an end-to-end fashion. Finally, the car-following data with multiple preceding vehicles captured from the NGSIM dataset are employed to train and calibrate the proposed model. Experimental results indicate that the deep learning-based models' performance in learning heterogeneous driving behavior can be enhanced by adding information about multiple preceding vehicles. In addition, the proposed ISDL model outperforms the benchmark car-following models in terms of the accuracy of the simulated speeds and simulated positions. Through tests on platoon simulation, the ISDL model is capable of reshaping the traffic oscillation phenomenon as well.

INDEX TERMS Car-following modeling, improved sequence-to-sequence model, information flow topology, gated recurrent unit neural network, connected automated vehicle.

I. INTRODUCTION

Car-following and behavior modeling describe the interaction relationship and the trend of motion between the host vehicle and its preceding vehicle in a lane [1]. Since the accuracy of car-following models plays a critical role in analyzing traffic state and making simulations, it is necessary to study the microscopic car-following models to further improve traffic safety and efficiency.

The associate editor coordinating the review of this manuscript and approving it for publication was Shajulin Benedict.

With the rapid development of perception and communication technology, connected and automated vehicle highway (CAVH) system [2] has become a development trend of intelligent transportation to relieve congestion and improve capacity. In a CAVH system, connected automated vehicles (CAV) are proposed to improve operational efficiency and reliability. Based on the Vehicle to Everything (V2X) communication system, the CAVs can not only capture the motion information from their surrounding vehicles but also transfer the real-time traffic state data with roadside units [3]. Hence, an effective car-following model is also

a significant technology for the CAVs to estimate traffic state and make decisions, which can help the CAVs to efficiently process information from more preceding vehicles ahead and better fit human driving behaviors under different scenarios.

Normally, microscopic car-following models can be divided into two categories, including the conventional model based on mathematical formulas [4], [5] and data-driven models [6]. Supported by high-fidelity traffic data and artificial intelligence technologies, deep learning-based models have become a main branch of the data-driven car-following models [7], [8], [9]. Though researchers have proposed various car-following models during the past few decades, some limitations still exist as follows.

(1) Most existing deep learning-based car-following models concentrate on using a recurrent neural network, such as the long short-term memory (LSTM) neural network [9] or the gated recurrent unit (GRU) neural network [8] to learn the memory effect and reaction delay of human driving characteristics. It is necessary to treat the car-following driving behavior as a sequence-to-sequence (Seq2seq) issue and extend the basic Seq2seq framework to improve the performance in generating the vehicle trajectory.

(2) The development of the communication technology promotes the information flow topology of CAVs, which are beneficial to improve the stability of controlling platoon of CAVs [10]. Though some deep learning-based car-following models have been proposed to fully consider reaction delay or memory effect in human driving behavior, few of them consider employing the complex information flow topology to improve the capability of deep learning structures in capturing heterogeneous driving behavior.

Since the multi-vehicle information interaction is fundamental for the CAVs and the present data-driven car-following models do not consider the influence of multiple preceding vehicles such as acceleration, speed, and space headways, this paper intends to propose a novel data-driven car-following model based on an improved Seq2seq deep learning (ISDL) framework. The proposed ISDL model employs the bidirectional GRU (Bi-GRU) structure and GRU structure as the encoder and decoder of the ISDL model respectively. In addition, the attention mechanism is introduced to extend the context vector in the decoder by extracting important information at each time interval. To fully capture the characteristics of the car-following behaviors, the kinematics parameters reflecting the status of the host vehicle and multiple preceding vehicles are utilized to form the input vectors of the proposed model. Based on the trajectory data of the Next Generation Simulation (NGSIM) data [11], the platoon trajectories containing the car-following behavior of multiple vehicles are extracted to train and calibrate the models. Experiments on empirical trajectories reveal that the new model yields significantly higher simulation accuracy and stability than existing car-following models in terms of speed prediction and position prediction. Furthermore, the proposed model is capable of capturing heterogeneous driving behaviors and reshaping the traffic oscillation in platoon simulation.

Based on the aforementioned description, the contributions of our work focus on the following aspects:

(1) The information flow topology containing motion parameters of preceding vehicles is integrated with a deep learning-based car-following model for the first time to capture heterogeneous driving behavior.

(2) A novel deep learning-based car-following (ISDL) model is constructed based on an improved Seq2seq structure by integrating the Bi-GRU encoder and attention-based decoder into an end-to-end fashion.

(3) Experiments on real-world trajectories data indicate the proposed ISDL model yields significantly high simulation accuracy in reproducing the car-following behavior, which outperforms the IDM model, GRU model, LSTM model and Seq2seq-based models in terms of speed prediction and position prediction.

(4) The proposed model is capable of conducting platoon simulations and reproducing the traffic oscillation phenomenon.

The rest of the paper is organized as follows. Section II summarizes the related work of microscopic car-following modeling from categories of model-driven models and data-driven models. Section III describes the methodology of the Seq2seq structure, GRU cell, and the framework of the proposed ISDL car-following model in detail. Section IV presents the dataset description, model implementation with baselines, and evaluation indexes. Section V provides the result discussion and analysis. Finally, the conclusion and outlook for future work are given in Section VI.

II. LITERATURE REVIEW

In this section, we review the work of microscopic car-following modeling by dividing the methods into model-driven models and data-driven models.

A. MODEL-DRIVEN CAR-FOLLOWING MODELS

Conventional model-driven car-following models usually use the dynamics method to study the influence of the motion state change of the preceding vehicle on the motion state of the host vehicle. By quantitatively analyzing the dynamic characteristics of ''preceding vehicle−host vehicle'' pairs in a lane, the formation and evolution mechanism of traffic phenomena such as traffic congestion and traffic oscillation can be studied [12].

Based on the prior knowledge of driving behavior, model-driven car-following models usually make specific assumptions about driving behavior, and they can be classified into many types including secure distance models (e.g. Gipps model [13] and FRESIM model [14]), psycho-physical models (e.g. Winsum model [15]), optimization velocity models (e.g. OVM model [16], GF model [17], and FVD model [18]), stimulus-response models (e.g. GHR model [19]

and Newell model [11]) and intelligent driving models (e.g. IDM model [20], [21]).

In general, model-driven car-following modeling depends on the physical methods or algebraic methods such as vehicle dynamics, and mathematical statistics, aiming at constructing models with practical physical and mathematical meanings. The advantage of model-driven car-following models lies in focusing on the several key elements that describe the physical properties of car-following behavior. However, these models extremely rely on mathematical formulas. Fine calibration of the formulae in the model is required before application. In addition, the randomness of the human driving behavior and the complexity of the road conditions make the parameter calibration often subject to large errors, and it is difficult to meet the needs of the future mixed operation of different types of vehicles in a CAVH environment.

B. DATA-DRIVEN CAR-FOLLOWING MODELS

1) ARTIFICIAL-BASED INTELLIGENT MODELS

The advent of the big data era has enabled researchers to obtain a large amount of high-precision real-time vehicle data, which in turn has driven the development of data-driven following models. Based on real-world vehicle driving data and machine learning methods, the data-driven following models are capable of exploring the inherent laws of car-following behavior by the training, learning, iteration, and evolution of sample data.

Wei et al. [22] proposed a self-learning support vector regression (SVR) method to study the asymmetric features in the following behavior and their impact on the traffic flow evolution, analyzing the time-lag phenomenon of stop-and-go waves at the microscope level and reproducing different congestion propagation patterns at the macroscope level. He et al. [23] proposed a K-nearest neighbor-based algorithm, which is used as the output of the model by finding K-similar driving scenarios in the historical vehicle trajectory database to obtain the most likely driving behavior. Kehtarnavaz et al. [12] introduced artificial neural networks (ANNs) to learn the feature of the car-following behaviors for the first time, and then many ANN models [24], [25], [26] have been built in this issue. Panwai and Dia [27] reveal that the BP artificial neural networks-based car-following model using the velocity and the headway of the preceding vehicle has a better performance than the Gipps model and the psychophysical models.

2) DEEP LEARNING-BASED MODELS

With the development of artificial intelligence, 5G communication technology, and data storage technology, the data-driven follow-through model gradually develops from machine learning models to deep learning model. As a frontier theory of machine learning technology, deep learning methods have been applied to build the data-driven car-following model by related scholars [28].

For example, Wang et al. [8] early verified that the recurrent neural network (RNN) method can significantly improve the trajectory fitting accuracy of the longitudinal trajectory than the traditional car-following models. Zhou et al [29] found that deep neural networks can not only fit the car-following trajectory well but also predict the traffic oscillation accurately. Huang et al. [9] considered asymmetric driving behaviors and proposed an LSTM-based car-following model. Experimental results indicate the proposed model is able to reproduce a variety of traffic flow characteristics significantly.

Besides, it also proved that the deep learning model-driven car-following model can not only fit the real driving trajectory well but also fully reflect the driving memory influence and response delay phenomenon. Lin et al. [30] proposed a formation following model based on the LSTM and scheduled sampling technique, which can effectively reduce the propagation of spatio-temporal errors. Hao et al. [31] proposed an encoder-decoder model based on GRU to recognize the driver's intention and forecast the trajectory of the vehicle. Though existing studies have shown that RNN-based deep learning models can effectively fit the following behavior of vehicles and reconstruct the following trajectory, the existing data-driven models do not fully consider the potential influence of multiple preceding vehicles on driving behavior.

III. METHODOLOGY

A. PRELIMINARIES

1) Seq2seq MODEL

Previous studies [7], [8], [9] have demonstrated that an RNN-based healing model can well fit the car-following trajectory and respond to the driver's response delay. The structures of the RNNs model can be divided into the one-to-one structure, one-to-many structure, many-to-one structure, and many-to-many structure. In the framework of a many-to-many structure, the input and output can be corresponding sequences.

Seq2seq [32] model is a classical RNN framework for handling many-to-many patterns, which has been widely used in fields such as machine translation [33], [34] and time series prediction [35], [36]. In the case of the car-following problem, the feature vectors formed by the variables of multiple preceding vehicles and host vehicles can be organized into input sequences according to time series, and the future states such as speed and acceleration of the host vehicles can generate used as output sequences.

The core architecture of the Seq2seq model is an encoder-decoder framework, which is composed of two RNN models as encoder and decoder respectively. In the encoding process, one RNN model acts as the encoder to compress the input sequence into a fixed-length context vector, and in the decoding process, another RNN acts as the decoder of this vector to output the corresponding sequence according to the context vector output in the encoding process and the input at the last moment. As shown in Fig.1, the Seq2seq framework consists

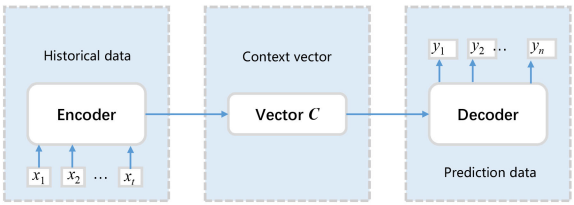

FIGURE 1. Diagram of the encoder-decoder structure.

of an encoder, a context vector, and a decoder. In the encoding stage, the input time series is $X_t = (x_1, x_2, \ldots, x_t)$. According to the data at different input moments, the hidden state of the encoder is described as:

$$h_t = f\,(X_t, h_{t-1}, x_t) \tag{1}$$

$$c = q\,(\{h_1, h_2, \ldots, h_t\}) \tag{2}$$

where h_t represents output of the hidden layer and c represents the context vector of the encoder. $f(.)$ and $q(.)$ are nonlinear functions. Based on related studies [31], $f(.)$ can be RNN-based function and $c = h_t$.

During the decoding process, the context vector is the initial hidden layer state of the decoder and the output prediction sequence is $Y = (y_1, y_2, \ldots, y_n)$. For the output at time interval t:

$$p(y_t|\{y_1, \ldots, y_{t-1}\}, c') = g(y_{t-1}, s_t, c) \tag{3}$$

$$p(Y) = \prod_{t=1}^{n} p(y_t|\{y_1, \ldots, y_{t-1}\}, c) \tag{4}$$

where $g(.)$ represents the RNN-based function and s_t is the hidden state at time interval t, $s_t = f(y_{t-1}, s_{t-1}, c)$. n represents the length of the output sequence.

Note that the Seq2seq model aims to maximize the conditional probability $p(Y)$ through training.

2) GRU STRUCTURE

RNN can deal with time series with length changes, and the input information of each layer depends on the output information of the previous layer and the previous information. To tackle the RNN's problem of gradient explosion or gradient disappearance when processing long-term data, gate recurrent unit (GRU) [37] is proposed to solve the gradient problem in long-term memory and backpropagation of the error.

Different from the LSTM unit which contains three gates including the input gate, forget gate, and output gate [38], the GRU units only have a reset gate r_i and an update gate z_i. The states of the two gates are determined by the hidden state h_{i-1} and input matrix x_i. Specifically, the reset gate selects the degree of information to remember from the input x_i. The update gate determines how much information to forget in h_{i-1} and how much information to remember in h_i'. Compared to the LSTM block, the structure of the GRU block is more simple with similar performance. Meanwhile, the GRU model is easy for training and the efficiency can be greatly improved. Hence, GRU structure is greatly used in natural language processing [39] and feature classification [40]. It has been also used in traffic condition estimation [41] and car-following behavior [8].

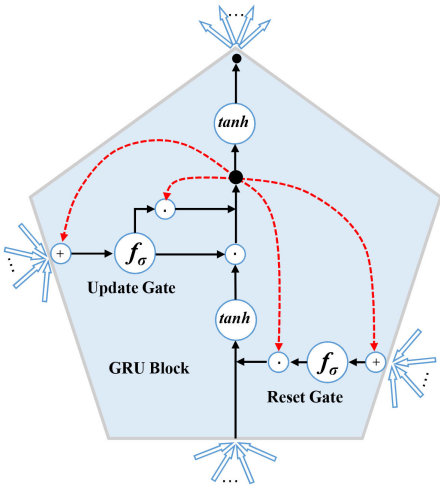

FIGURE 2. The structure of GRU block.

The network structure of the GRU model is shown in Fig.2, and the calculation formula of the model is as follows:

$$z_i = \sigma(W_z x_i + U_z h_{i-1}) \tag{5}$$

$$r_i = \sigma(W_r x_i + U_r h_{i-1}) \tag{6}$$

$$h_i' = \tanh(W_h x_i + U_h[r_i \circ h_{i-1}]) \tag{7}$$

$$h_i = (1 - z_i) \circ h_{i-1} + z_i \circ h_i' \tag{8}$$

$$y_i = \sigma(W_y h_i) \tag{9}$$

where σ_s and $\circ$ define the sigmoid function and the scalar product of two vectors. W_z, U_z, W_r, U_r, W_h, U_h and W_y are weights and biases. The sigmoid activation function $\sigma(.)$ and function tanh(.) are shown as follows.

$$\sigma(x) = \frac{1}{1 + e^x} \tag{10}$$

$$\tanh(x) = \frac{e^x - e^{-x}}{e^x + e^{-x}} \tag{11}$$

where the sigmoid function maps the value into range (0, 1) and the tanh function maps the values between -1 and 1.

B. CAR-FOLLOWING MODEL BASED ON IMPROVED Seq2seq DEEP LEARNING MODEL

To give full consideration to the potential impact of various information on driving behavior and develop an intelligent model for describing connected driving in the future, this paper proposes a car-following model based on deep Seq2seq learning framework. Firstly, we consider the potential influence of multiple preceding vehicles' information on the car-following behavior of the host vehicle [42]. Secondly, an improved Seq2seq framework, which employs the bidirectional GRU and one-way GRU model as the encoder

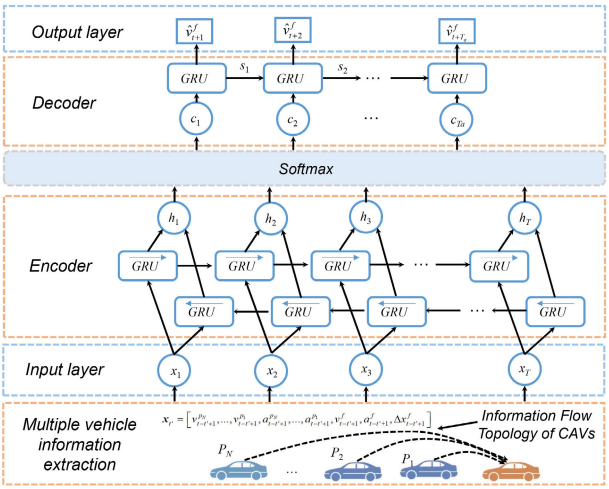

FIGURE 3. The framework of the ISDL model.

and decoder, is proposed for extracting and learning the car-following behavior. To better extract the information and assign appropriate weights to important hidden states, this model introduces the attention mechanism to generate the different context vectors at each time interval. Fig.3 provides the framework of the ISDL model.

1) FEATURES EXTRACTION AND MODEL INPUT

Donate p_i as the i-th preceding vehicles of the host vehicle, $i = 1, 2, \ldots, N_p$, where N_p is the number of the preceding vehicles. Let $v_t^{p_i}$ represent the speed of i-th preceding vehicle at the time interval t and $a_t^{p_i}$ represent the acceleration of the i-th preceding vehicle at the time interval t. In addition, v_t^f and a_t^f represent the speed and acceleration of the host vehicle at time interval t. Δx_t^f is the space headway between the nearest preceding vehicle and the host vehicle. To estimate the speed of host vehicle at time interval $t+1$, the vector of input matrix at time interval t' can be written as:

$$x_{t'} = [v_{t-t'+1}^{p_N}, \ldots, v_{t-t'+1}^{p_1}, a_{t-t'+1}^{p_N}, \ldots, a_{t-t'+1}^{p_1}, v_{t-t'+1}^{f}, a_{t-t'+1}^{f}, \Delta x_{t-t'+1}^{f}] \tag{12}$$

The input matrix of the Seq2seq model is given as:

$$X_t = [x_T, x_{T-1}, \ldots, x_{t'}, \ldots, x_1]^T \tag{13}$$

where T indicates the length of the input timestep, which can be recognized as the length of the memory when the host vehicle follows the preceding vehicles.

2) BiGRU-BASED ENCODER

To better employ past and future driving information to capture the characteristics of the following behavior in the matrix, the proposed ISDL model proposes a bidirectional GRU structure to process driving information.

To be specific, the forward states of the bidirectional GRU neural network (BiRNN) are computed:

$$\vec{h}_t = (1 - \vec{z}_t) \circ \vec{h}_{t-1} + \vec{z}_t \circ \vec{h}'_t \tag{14}$$

where

$$\vec{h}'_t = \tanh\left(\vec{W}_h X_t + \vec{U}_h \left[\vec{r}_t \circ \vec{h}_{t-1}\right]\right) \tag{15}$$

$$\vec{z}_t = \sigma\left(\vec{W}_z X_t + \vec{U}_z \vec{h}_{t-1}\right) \tag{16}$$

$$\vec{r}_t = \sigma\left(\vec{W}_r X_t + \vec{U}_r \vec{h}_{t-1}\right) \tag{17}$$

X_t is the input matrix of the driving behavior. $\vec{W}_h$, $\vec{W}_z$, $\vec{W}_r$, $\vec{U}_h$, $\vec{U}_z$, and $\vec{U}_r$ are weight matrices of the forward GRU. The backward state $\left(\overleftarrow{h}_1, \overleftarrow{h}_2, \ldots, \overleftarrow{h}_T\right)$ are computed similarly. The embedding input matrix are shared between the forward and backward RNNs, unlike the weight matrices. We concatenate the forward and backward states to obtain the annotations $(h_1, h_2, \ldots, h_T)$, where

$$h_t = [\vec{h}_t; \overleftarrow{h}_t] \tag{18}$$

3) ATTENTION-BASED DECODER

In a conventional encoder-decoder framework used in the car-following model proposed by Ma et al. [43], the encoder converts the input sequence into the semantic vector of the same compression length and the context vectors of the decoder at different time intervals are the same. Since the feature distribution of sequence data is different, the importance of its influence on the output is also different. To prevent the information input first from being diluted by the information input later when processing long sequences, this paper introduces an attention mechanism in the hidden layer to make the input of the decoder adopt different intermediate semantics c. Each c is calculated by weight a and encoder hidden layer output of the Bi-GRU h. Since different values are given corresponding weights, important features can be captured according to the impact degree of the input sequence, and the hidden state obtained by the encoder under the Bi-GRU structure is calculated as $(h_1, h_2, \ldots, h_T)$.

If the current hidden layer state of the decoder is s_{t-1}, the correlation between each input position $j, j = 1, 2 \ldots, T$ and the current output position is calculated asiij$\check{Z}$

$$e_{tj} = \theta\left(s_{t-1}, h_j\right) \tag{19}$$

The Eq.19 can also be written as:

$$e_{tj} = {v_a}^T \tanh\left(W_a s_{t-1} + U_a h_j\right) \tag{20}$$

where v_a, W_a and U_a represent the weights of the correlation function $\theta(.)$.

The context vector c_t of t-th prediction time interval, $t = 1, 2, \ldots, T_a$ is computed as:

$$c_t = \sum_{j=1}^{T} \alpha_{tj} h_j \tag{21}$$

$$\alpha_{tj} = \frac{exp(e_{tj})}{\sum_{k=1}^{T_x} exp(e_{tk})} \tag{22}$$

where α_{tj} represents the weight of the hidden state h_j on the context vector c_t.

The hidden state s_i of the decoder given the annotations from the encoder is computed by

$$s_t = (1 - z_t) \circ s_{t-1} + z_t \circ s_t' \tag{23}$$

where

$$s_t' = \tanh\left(W_s y_{t-1} + U_s\left[r_t \circ s_{t-1}\right] + W_c c_t\right) \tag{24}$$

$$z_t = \sigma\left(W_{z'} y_{t-1} + U_{z'} s_{t-1} + C_z c_t\right) \tag{25}$$

$$r_t = \sigma\left(W_{r'} y_{t-1} + U_{r'} s_{t-1} + C_r c_t\right) \tag{26}$$

where W_s, $W_{z'}$, $W_{r'}$, U_s, $U_{z'}$, $U_{r'}$, W_c, C_z and C_r are the weights of the decoder.

4) OUTPUT AND LOSS FUNCTION

The output of the improved Seq2seq framework is the speeds of the host vehicle in future periods $V = [\hat{v}^f_{t+1}, \hat{v}^f_{t+2}, \ldots, \hat{v}^f_{t+T_a}]$. For the output at a future time interval, the predicted speed $\hat{v}^f_{t+\Delta t}$, $\Delta t = 1, 2, \ldots, T_a$ it can be written as:

$$p\left(\hat{v}^f_{t+\Delta t} \middle| \hat{v}^f_{t+1}, \ldots, \hat{v}^f_{t+\Delta t-1}, X_t\right) = g\left(\hat{v}^f_{t+\Delta t-1}, s_{\Delta t}, c_{\Delta t}\right) \tag{27}$$

The loss function, namely the objective function, is used to calculate the error between the predicted value and the real value. Considering that the optimization of only one variable may lead to abnormalities [20], this paper adopts the dual objective of speed and displacement as the loss function. Normalized data with the mean square error is used to calculate errors between the simulated trajectory and the observed trajectory.

The objective function is:

$$L_{\mathrm{MSE}} = \frac{1}{N_k}\sum_{k=1}^{N_k}\left(\hat{v}^f_k - v^f_k\right)^2 + \frac{1}{N_k}\sum_{k=1}^{N_k}\left(\hat{x}^f_k - x^f_k\right)^2 \tag{28}$$

where L_{MSE} is the mean square error function. N_k represents the number of training data. $\hat{v}^f_k$ and v^f_k represent predicted speeds and measured speeds. $\hat{x}^f_k$ and x^f_k represent predicted positions and measured positions.

The pseudo-code of training an ISDL model is presented in Table 1.

TABLE 1. Pseudo-code of training an ISDL model.

Algorithm: The training process of the ISDL model
Input: The number of the preceding vehicles N_p, the length of the input timestep T
Output: A trained ISDL model
Initialize a null set: $\Omega \leftarrow \varnothing$
For the following vehicles which have N_p preceding vehicles $f(1 \le f \le F)$ do
  For all available time intervals $t(1 \le t \le ep)$ do
    For t= 1 to T do
      $x_{t'} \leftarrow [v^{pN}_{t-t'+1}, \ldots, v^{p1}_{t-t'+1}, a^{pN}_{t-t'+1}, \ldots, a^{p1}_{t-t'+1}, v^{f}_{t-t'+1}, a^{f}_{t-t'+1}, \Delta x^{f}_{t-t'+1}]$
    End for
    $X_t \leftarrow [x_T, x_{T-1}, \ldots, x_{t'}, \ldots, x_1]$
    $V_t \leftarrow [\hat{v}^f_{t+1}, \hat{v}^f_{t+2}, \ldots, \hat{v}^f_{t+T_a}]$
    A training observation (X_t, V_t) is put into Ω
  End for
End for
Initialize all the weights and biases
Repeat
  Randomly sample a mini-batch sample Ω_b from Ω
  Estimate the parameters by minimizing the Eq.28 within Ω_b
Until convergence criterion met

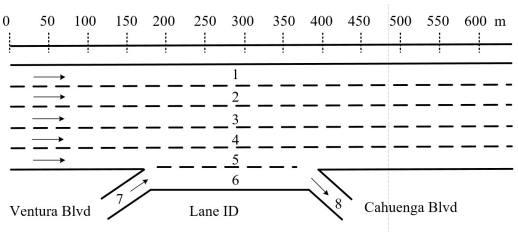

FIGURE 4. The schematic diagram of road segments on U.S. Highway 101 in the NGSIM dataset.

IV. EXPERIMENT

A. DATA PREPARATION

To validate the performance of the proposed model, the sdata[1] of the NGSIM [44] project are adopted to prepare the experimental dataset. The original NGSIM data are collected in form of images by camera equipment with 0.1 s time interval. Trajectory data of vehicles on the US - 101 highway road shown in Fig.4 are extracted including the exact location information of each vehicle. The dataset is large and highly accurate, which can satisfy the testing requirements for training deep learning-based models under car-following scenarios, especially multi-vehicle car-following behaviors containing complex information flow topology. Note that the extracted car-following data only consider the impact of multiple preceding vehicles in a lane on the host vehicle without considering the surrounding vehicles in other lanes.

According to relevant research, high traffic volume usually occurs during the morning rush hour of US-101 from 8:05 am to 8:20 am, leading to the phenomenon of multiple car-following behaviors and traffic oscillation. Hence, the dataset during the period above is taken as the basic dataset. Through data preprocessing, 621 groups of car-following pairs with two preceding vehicles are selected including 461 groups of data for training and validation and other 160 groups of data for testing. During the process of model testing, the well-trained deep learning-based car-following models predict the speeds of the host vehicle according to the speeds and accelerations of the host vehicle and the preceding vehicles, and the relative position between the host vehicle and the nearest preceding vehicle. In addition, the predicted position of the vehicle can be calculated as:

$$\hat{d}^f_{t+1} = \frac{1}{2}(\hat{v}^f_t + \hat{v}^f_{t+1})\Delta t \tag{29}$$

[1] https://catalog.data.gov/dataset/next-generation-simulation-ngsim-vehicle-trajectories-and-supporting-data

where $\hat{v}_t^f$ and $\hat{v}_{t+1}^f$ present the traffic speeds of the predicted vehicle speed at a time interval t and $t+1$. Δt is the time interval and $\Delta t = 0.1s$.

The experimental environment is a DELL computer (Inter Core I7-10750h CPU, 32G RAM). The Keras high-level neural network API in Tensorflow is used as the framework, and the model is built and trained in Python 3.7 to evaluate the prediction performance of the model.

B. BENCHMARK MODELS

To estimate the capability of reshaping car-following of the proposed model, we compared it with the IDM model [45], the LSTM model [9], the GRU model [8], the Seq2seq deep learning (SDL) model [43] and GRU-based SDL (GSDL) model [31].

IDM: IDM model is a classic accident-free theoretical following model, which has clear physical significance and can intuitively display the changes in driving behavior. In addition, this model can describe the following behavior of single-lane vehicles under free flow and congested flow at the same time. All model parameters have clear physical meanings, which can intuitively display the changes of driving behavior. The specific expressions are as follows:

$$a_{t+1}^f = \tilde{a}\left[1 - \left(\frac{v_t^f}{\tilde{v}}\right)^4 - \left(\frac{S*\left(v_t^f, \Delta v_t^f\right)}{\Delta s_t}\right)^2\right] \tag{30}$$

$$S^*\left(v_t^f, \Delta v_t^f\right) = s_0 + t_0 v_t^f - \frac{v_t^f \Delta v_t^f}{2\sqrt{\tilde{a}\tilde{b}}} \tag{31}$$

where $S^*\left(v_t^f, \Delta v_t^f\right)$ is the desired spacing function, which is determined by the speed of the host vehicle v_t^f and speed difference Δv_t^f, $\Delta v_t^f = v_t^f - v_t^p$. $\tilde{v}$ is the expected speed. $\tilde{a}$ is the maximum acceleration and $\tilde{b}$ is the maximum deceleration. s_0 and t_0 represent the minimum safe spacing and desired headway.

According to the data of the host vehicle and the preceding vehicle in the training set, relevant parameters of the IDM model are calibrated, and the calibrated data can be obtained as shown in Table 2.

TABLE 2. Parameter calibration results of IDM model.

Parameters	Unit	Values
$\tilde{v}$	m/s	29.05
$\tilde{a}$	m/s^2	2.83
$\tilde{b}$	m/s^2	2.02
t_0	s	1.62
s_0	m	7.09

LSTM: The LSTM-based car-following model is proposed by [9] according to the architecture of the LSTM structure. The kinematics states of the host vehicles and preceding vehicles are formed as the input of the LSTM model. Besides, the number of the hidden layer of the LSTM car-following model is selected as 1.

GRU: The GRU-based car-following model used the basic GRU structures described in Section IV-B, and there is one hidden layer in the model [8].

SDL: The first Seq2seq deep learning (SDL) model for modeling the car-following behavior is given by Ma et al. [46]. The SDL model employs the LSTM as the encoder and decoder with the numbers of hidden layers both set as 1.

GSDL: A GRU-based Seq2seq deep learning (SDL) model is also employed as a baseline model. It is built according to Hao's study [31]. The GSDL uses a one-way GRU layer as the encoder and another one-way GRU layer with an attention mechanism as a decoder.

To fairly compare the performance of different models, the number of training epochs and the batch size are chosen as 50 and 64 for all deep learning-based models including the LSTM model, GRU model, SDL model, GSDL model, and ISDL model. The optimizer of the model is chosen as Adam with the learning rate set as 0.0001, and the number of hidden units in the hidden layer of all deep learning-based car-following models is set as 128. In addition, the training will be stopped automatically if the loss function of the training data set is not improved in 10 consecutive training sessions. Since the number of the preceding vehicles determines the amount of information that is used to capture the car-following behavior, the deep learning-based car-following models will consider the same number of the preceding vehicles to extract kinematics states as the input of these models.

C. EVALUATION CRITERIA

In this paper, the mean absolute error of the predicted velocity (MAE_v) and predicted position (MAE_x) are selected as evaluation indexes. To better evaluate the error of the trajectory simulation, the mean squared error of the predicted position (MSE_x) is introduced as the evaluation indexes as well. The calculation equations for these indexes are revealed as follows:

$$\text{MAE}_v = \frac{1}{N_s}\sum_{i=1}^{N_s}\frac{1}{L_i}\sum_{j=1}^{L_i}\left|\hat{v}_{i,j}^f - v_{i,j}^f\right| \tag{32}$$

$$\text{MAE}_x = \frac{1}{N_s}\sum_{i=1}^{N_s}\frac{1}{L_i}\sum_{j=1}^{L_i}\left|\hat{x}_{i,j}^f - x_{i,j}^f\right| \tag{33}$$

$$\text{MSE}_x = \frac{1}{N_s}\sum_{i=1}^{N_s}\frac{1}{L_i}\sum_{j=1}^{L_i}\left(\left|\hat{x}_{i,j}^f - x_{i,j}^f\right|\right)^2 \tag{34}$$

where N_s is the number of vehicles in the testing dataset. L_i defines the lengths of the trajectories of i-th vehicle. $\hat{v}_{i,j}^f$ and $v_{i,j}^f$ denote simulated speeds and empirical speeds of the i-th vehicle at the j-th points of trajectories. $\hat{x}_{i,j}^f$ and $x_{i,j}^f$ denote the simulated position and empirical position of the i-th vehicle at the j-th points of trajectories.

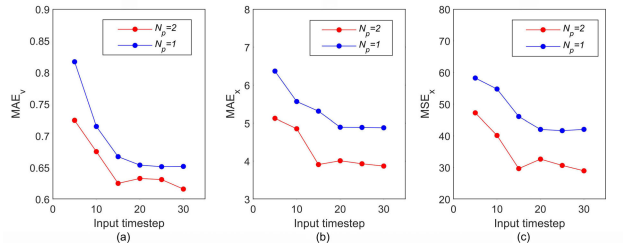

FIGURE 5. The influence of the input timestep on the ISDL model. (a) MAE_v; (b) MAE_x; (c) MSE_x.

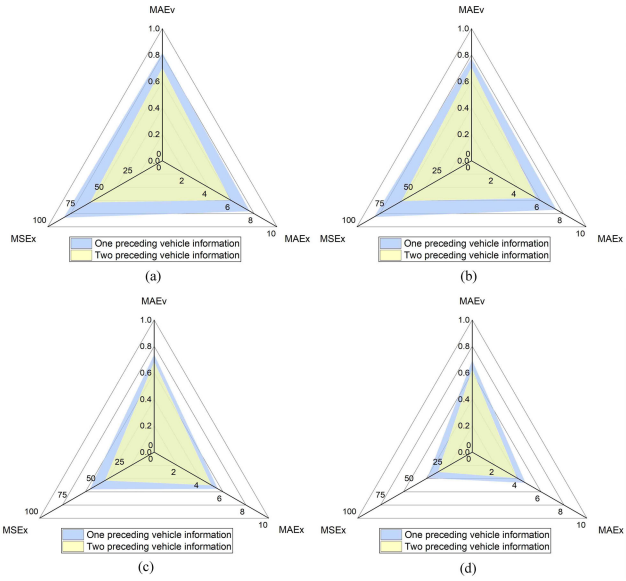

FIGURE 6. Comparison of the models with different information topology. (a) LSTM model; (b) GRU model; (c) SDL model; (d) ISDL model.

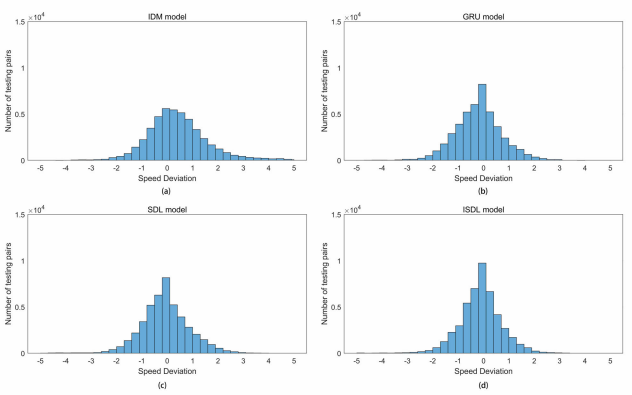

FIGURE 7. Empirical distributions of deviations between empirical speeds and simulated speeds of different models. (a) IDM model; (b) GRU model; (c) SDL model; (d) ISDL model.

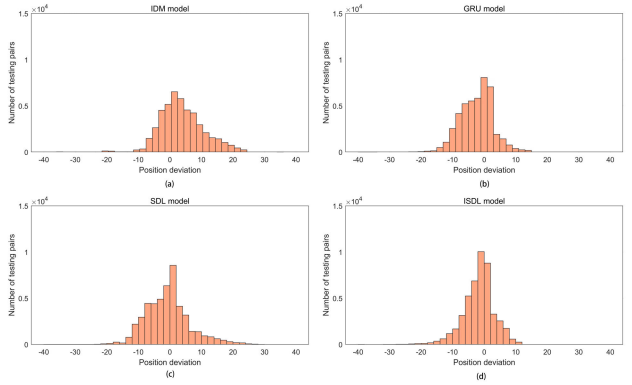

FIGURE 8. Empirical distributions of deviations between empirical position and simulated position of different models. (a) IDM model; (b) GRU model; (c) SDL model; (d) ISDL model.

V. RESULT AND DISCUSSION

A. INFLUENCE OF THE CRITICAL PARAMETER ON THE ISDL MODEL

The driving decision in the car-following process is closely related to the historical driving behaviors and the reaction delay of vehicles. As a common feature of human driving vehicles, the reaction delay consists of human psychological processing time, device response time, and vehicle movement time [47]. Previous studies indicate that the length of the input timestep considering the reaction delay affects the performance of the deep learning models [8], [9]. Papathanasopoulou et al. [48] indicate the reaction delay in a wide range from 0.4 s to 3.0 s and Zheng et al. [24] demonstrate that the minimum value of reaction delay is around 0.5 s. With the time interval of collecting the kinematics information set as 0.1 s, it is necessary to learn the length of the timestep on the performance of the ISDL by selecting the length of the timestep from [5], [10], [15], [20], [25], and [30], which corresponds to reaction delay from 0.5 s to 3.0 s with a step of 0.5 s.

Fig.5 indicates the performance of the ISDL model with input timestep ranging from 5 to 30 under the scenario $N_p = 1$ where the host vehicle generates a trajectory simulated by using the information of one nearest preceding vehicle in the scenario $N_p = 2$ where the kinematics parameters of two nearest preceding vehicles are employed to generates simulated trajectory. As indicated in Fig.5, the simulated speed error and simulated position error of the ISDL model decrease gradually with the input timestep increasing from 5 to 15. After the input timestep is larger than 15, the MAE_v, MAE_x, and MSE_x are stable with little fluctuation under the two scenarios. Hence, the optimal input timestep of the ISDL model is set as 15 and it is equal to 1.5 s. Note that with the same input timestep, the ISDL model considering two preceding vehicles' state information works better than the other with only one preceding vehicle's state information, indicating that the multiple vehicle information is a benefit to improving the predictive quality of simulated trajectories.

Considering the fact that the development of communication technology promotes the application of the CAVs, it is necessary to learn the influence of the information of the

TABLE 3. Comparison of the overall performance of different models in speed and position prediction.

Models	MAE_v	MAEv Reduction	MAE_x	MAE_x Reduction	MSE_x	MSE_x Reduction
IDM	1.033	–	8.21	–	108.36	–
GRU	0.700	32.29%	5.92	27.86%	62.74	42.11%
LSTM	0.703	31.93%	5.62	31.54%	60.91	43.79%
SDL	0.680	34.19%	4.99	39.19%	42.75	60.55%
GSDL	0.667	35.42%	4.57	44.28%	35.20	67.51%
ISDL	0.625	39.53%	3.91	52.37%	29.65	72.64%

multiple vehicles on the performance of deep learning-based models. Fig.6 compares the MAE_v, MAE_x, and MSE_x of the LSTM model, GRU model, SDL model, and ISDL model with different input features. It is displayed in Fig.6 that these models with two preceding vehicle information are superior to those with only one preceding vehicle information in terms of speed prediction and position prediction, indicating that the extra kinematics parameters provided by the second preceding vehicle are beneficial for fitting the behavior of the host vehicle. For each deep learning-based car-following model, the improvements in the simulated position are more significant than those in the simulated speed. Note that all deep learning-based car-following models organized their input matrix with two preceding vehicle information in the next sections.

B. COMPARISON OF THE PERFORMANCE OF DIFFERENT MODELS

In this section, we compare the overall performance of the ISDL model with those of the IDM, the LSTM, the GRU, the GSDL, and the SDL model. To achieve a fair contrast, the input timesteps of the deep learning-based model are set as 15. Table 3 presents the overall error indexes of different car-following methods. The proposed ISDL model works best among these models, which outperforms the second-best simulator GSDL model with the improvement of 0.042 and 5.55 on MAE_v and MSE_x. This may be caused by the fact that the ISDL proposes an improved sequence-to-sequence framework that employs a Bi-GRU encoder to better extract input from multiple preceding vehicle information. It can be found that the GSDL outperforms the SDL model with an improvement of 7.55 on MSE_x since it extends the Seq2seq framework with an attention mechanism to generate a context vector at each simulated time interval. Compared to the SDL and the GSDL model, the ISDL model is capable of learning the car-following behavior more effectively with the improved Seq2seq framework.

Besides, the deep learning-based models with Seq2seq frameworks have smaller errors on both simulated speed and positions since the Seq2seq is able to take memory effect and reaction into account [43]. The SDL model outperforms the LSTM model with improvements of 0.63 and 18.16 on MAE_x and MSE_x respectively. Meanwhile, Table 3 demonstrates that the deep learning-based model provides higher quality simulated results than the IDM model in fitting the following behavior since the data-driven models have more parameters to capture the heterogeneous following behavior from a large dataset.

To study the model performance of models under different states, we divide the car-following dataset into three sub-datasets including the low-speed car-following scenario, medium-speed car-following scenario, and high-speed car-following scenario, which correspond to the speeds below 7 m/s, speeds from 7 m/s to 12 m/s, and speeds more than 12 m/s. Table 4, Table 5, and Table 6 indicate the performance comparison of different models under the above scenarios. As shown in Table 4 when the vehicle follows at low speeds, the deep learning-based models have superior performance than the IDM model, and the ISDL model outperforms the SDL model with improvements of 14.44% and 21.83% on MAE_x and MSE_x respectively. It reveals that the ISDL model is capable of fitting the short headway of the car-following under the low-speed scenario. In addition, it is indicated in Table 5 and Table 6, the Seq2seq models present lower speed prediction and position prediction than other models, which demonstrates that the Seq2seq structure can well memory the driving behavior in medium-speed and high-speed car-following behavior.

Fig.7 and Fig.8 present the simulated error distribution of speeds and position respectively for four representative models including the IDM model, GRU model, SDL model, and ISDL model. It can be learned from Fig.7 that the four models all can provide accurate simulated speed while the simulated speed values present different distribution characteristics. Since the IDM is a classical following model driven by traffic safety, it generates the simulated speeds less than the empirical data with high frequency to guarantee safe space headway. While the GRU, the SDL, and the ISDL model prefer to generate simulated speeds a little larger than the empirical data to make the trajectory of the host vehicle closer to that of the preceding vehicle. In addition, the error distribution of the simulated speeds in Fig.7 reveals that the errors of the GRU, the SDL, and the ISDL model are more concentrated and near the mean values, illustrating that deep learning-based models can reshape the driving behavior better than the IDM model.

Similar to the phenomenon indicated in Fig.7, Fig.8 shows the error distribution of simulated positions of the four models. It can be distinctly found that the Seq2seq-based model behaves more accurately than the IDM and GRU model in tracking the leading vehicles. Meanwhile, the distribution of big errors of the SDL which are smaller than -10 and

TABLE 4. Performance comparison of the models under low-speed car-following scenarios.

Models	MAE_v	MAEv Reduction	MAE_x	MAE_x Reduction	MSE_x	MSE_x Reduction
IDM	0.974	–	5.79	–	65.02	–
GRU	0.774	20.54%	5.09	12.09%	44.63	31.36%
LSTM	0.777	20.26%	5.08	12.23%	40.13	38.28%
SDL	0.730	25.02%	4.58	20.83%	28.42	56.29%
GSDL	0.673	30.86%	3.89	32.74%	24.32	62.59%
ISDL	0.658	32.42%	3.54	38.86%	19.01	70.76%

TABLE 5. Performance comparison of the models under medium-speed car-following scenarios.

Models	MAE_v	MAEv Reduction	MAE_x	MAE_x Reduction	MSE_x	MSE_x Reduction
IDM	0.983	–	7.94	–	88.54	–
GRU	0.643	34.53%	5.37	32.38%	59.43	32.88%
LSTM	0.651	33.81%	5.20	34.57%	57.35	35.23%
SDL	0.638	35.05%	4.55	42.66%	40.25	54.55%
GSDL	0.607	38.20%	3.73	53.06%	29.92	66.20%
ISDL	0.590	39.94%	3.44	56.70%	25.26	71.47%

TABLE 6. Performance comparison of the models under high-speed car-following scenarios.

Models	MAE_v	MAEv Reduction	MAE_x	MAE_x Reduction	MSE_x	MSE_x Reduction
IDM	1.155	–	10.01	–	125.57	–
GRU	0.678	41.28%	6.77	32.30%	86.03	31.49%
LSTM	0.684	40.79%	6.64	33.63%	86.36	31.23%
SDL	0.664	42.49%	5.78	42.22%	54.68	56.46%
GSDL	0.655	43.28%	5.33	46.77%	51.28	59.16%
ISDL	0.622	46.14%	5.08	49.24%	48.84	61.11%

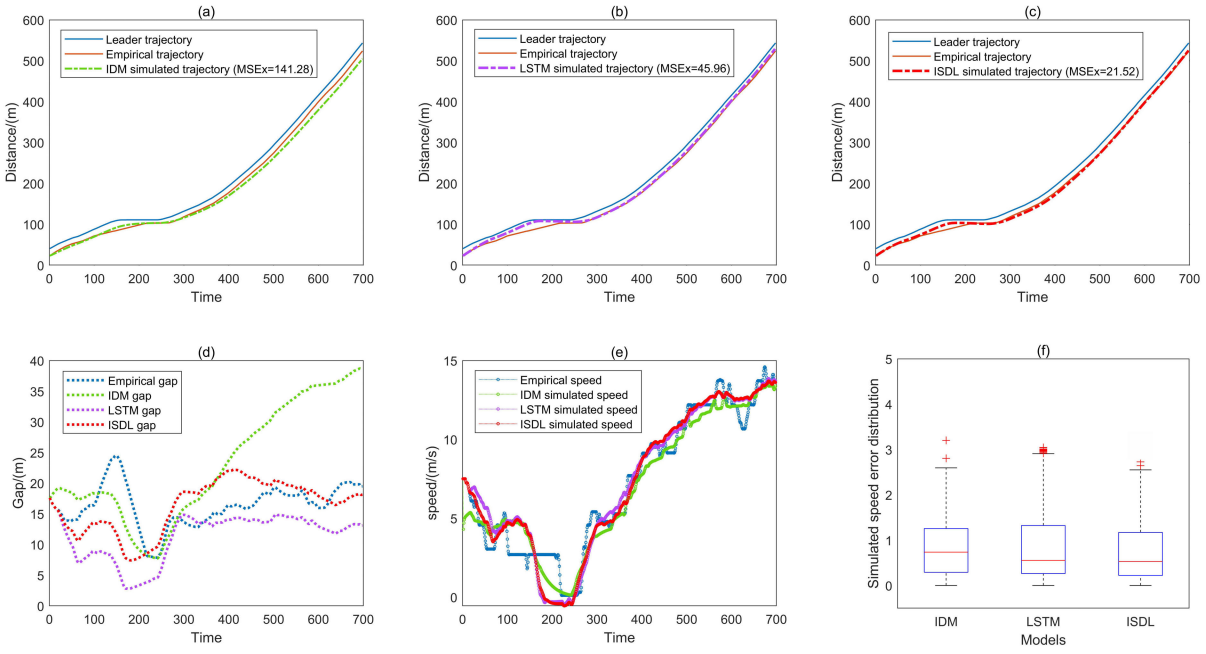

FIGURE 9. Performance of the models under regular driving behavior. (Vehicle 915 with an average gap distance 16.60 m).

larger than 10 are more frequent than those of the ISDL model, indicating that the ISDL model not only inherits the features of the SDL model in sequence learning but also improves its performance by introducing attention mechanism and bidirectional encoder to extract important information.

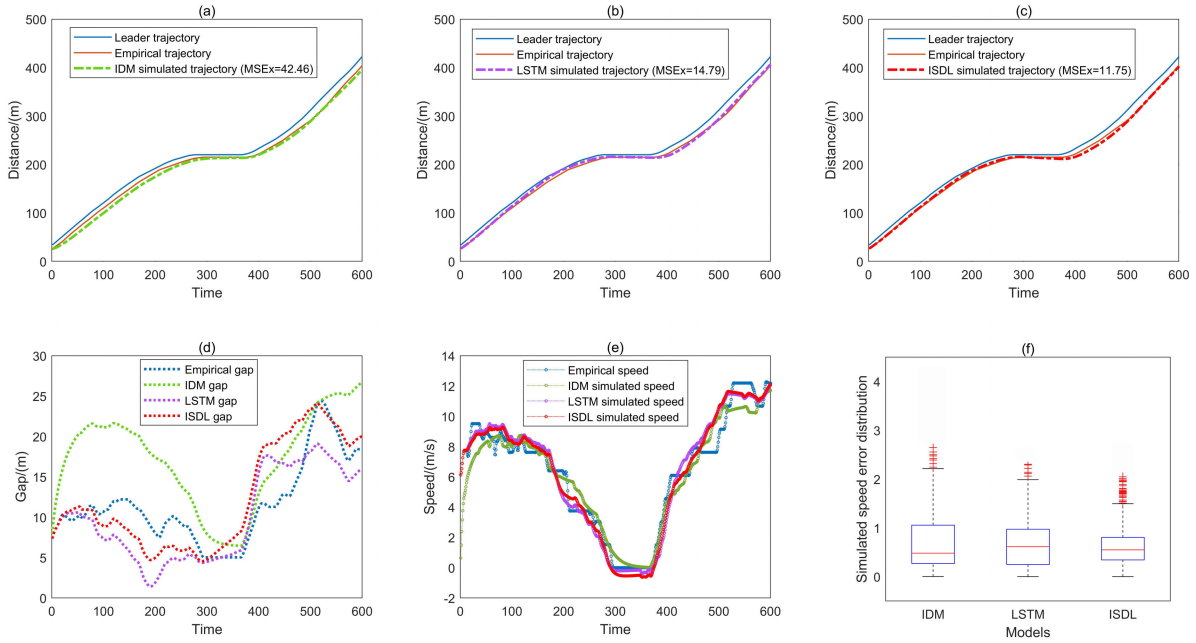

FIGURE 10. Performance of the models under aggressive driving behavior. (Vehicle 796 with an average gap distance 9.75 m).

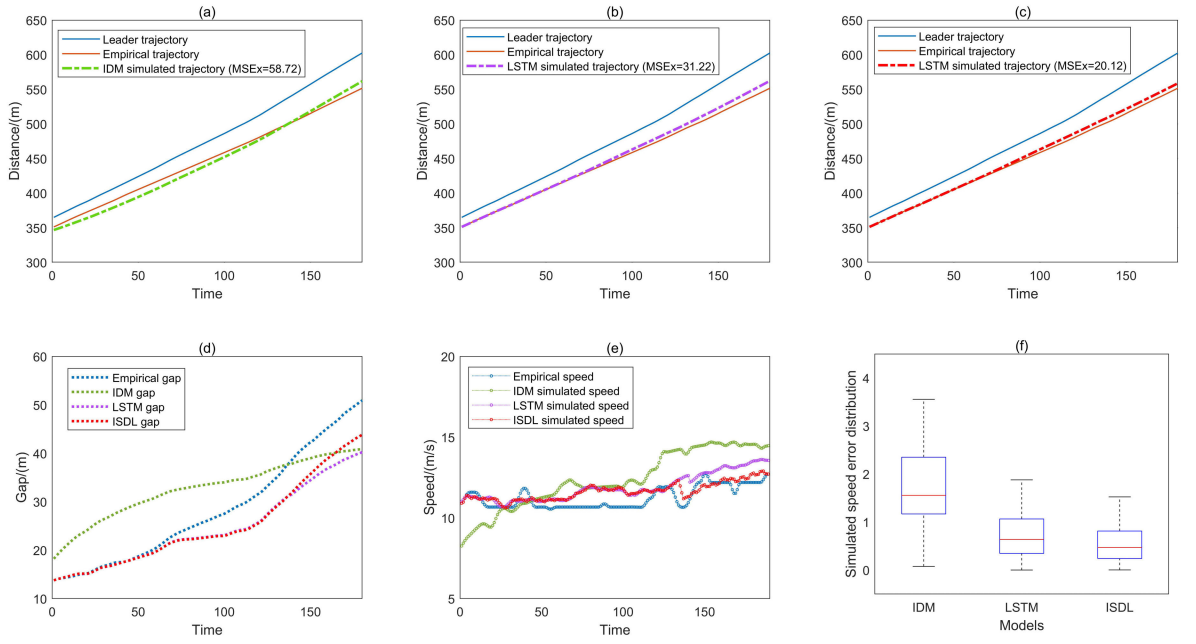

FIGURE 11. Performance of the models under cautious driving behavior. (Vehicle 965 with an average gap distance 28.91 m).

Furthermore, to investigate the performance of the models under heterogeneous driving behaviors, the simulated trajectories and the corresponding simulated speeds of the representative vehicles are presented. Note that we divided the behavior of the driver into three types including regular behavior, aggressive behavior, and cautious behavior according to related studies [49]. The aggressive driver tends to anticipate traffic conditions in advance and prefers to choose a smaller gap to follow the leader, which may cause traffic oscillation or stop-and-go traffic [50]. On the contrary, the

cautious driver always intends to keep a large distance from the preceding vehicle.

Fig.9, Fig.10, and Fig.11 present the performance of the models under the regular, aggressive, and cautious driving behavior respectively, which are distinguished according to the average gap distances of the trajectories. As shown in Fig.9, Fig.10, and Fig.11 where vehicle 915, vehicle 796, and vehicle 965 are in regular, aggressive, and cautious driving behavior, the IDM, LSTM, and ISDL model show different performance in simulating the following trajectories. Among the three models, the simulated trajectories of the ISDL model are closest to the empirical trajectories under three driving behaviors. Fig.9 indicates that the simulated speeds for regular driving behavior provided by the IDM, the LSTM, and the ISDL reveal comparable accuracy. Meanwhile, it can be observed in Fig.10 and Fig.11 that the LSTM and the ISDL model have much stronger performance than the IDM for aggressive and cautious driving behaviors. Note that the IDM model prefers to keep a larger gap than the LSTM model and ISDL model, which indicates that the deep learning models are capable of accurately generating simulated trajectories.

C. DETAILED BEHAVIOR COMPARISON AND PLATOON SIMULATION

Fig.12 investigates the detailed following behavior of different models. Considering that human drivers cannot accurately judge the speed of the leading vehicle or precisely maintain their speed, the relative spacing and speed between any two consecutive vehicles are usually oscillating. To further compare the accuracy of different kinds of models, it is necessary to get the oscillating behavior of different models by analyzing the driving behavior of specific vehicles. Fig.12 shows the condition where vehicle 865 follows vehicle 860, and provides the empirical data and simulation of the IDM model, LSTM model, and ISDL model. It is indicated that the ISDL model yields a more accurate approximation of the oscillating behavior than the IDM model and LSTM model.

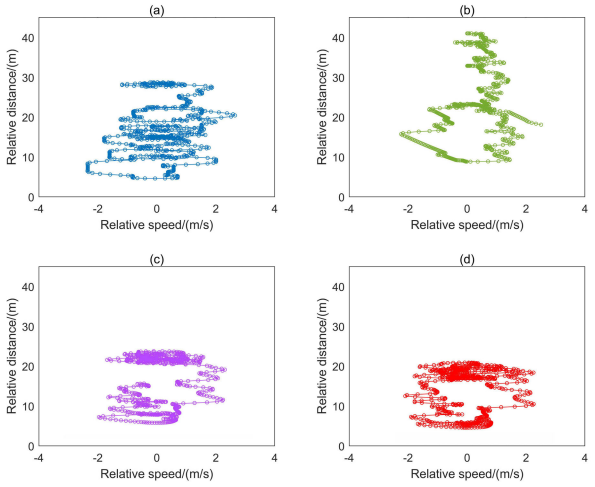

FIGURE 12. The scatter diagram of relative distances and speeds replicated by different models. (a) Empirical data; (b) IDM model; (c) LSTM model; (d) ISDL model.

Platoon simulation can reflect traffic phenomena such as oscillation and hysteresis, and it is a crucial application and indicator of car-following models. In the platoon simulation, the leading vehicle runs on a preset route, influenced by the instructions or the traffic states outside the platoon. Other vehicles run based on the car-following models. The movement of vehicles is affected by two preceding vehicles and their previous states except for the second vehicle, which has only one preceding vehicle. To further explore the performance of the proposed model in reproducing traffic oscillation, we extract a platoon that traverses stop-and-go waves for platoon simulation and the two leader vehicle are 739 and 745. Fig.13 presents the time-space diagrams of the real and simulated trajectories, indicating that the proposed model can estimate the traffic oscillations through platoon simulation. Though errors of the simulated accumulate from the upstream to downstream, the stop-and-go waves with accurately predicted speeds are well captured by the ISDL model.

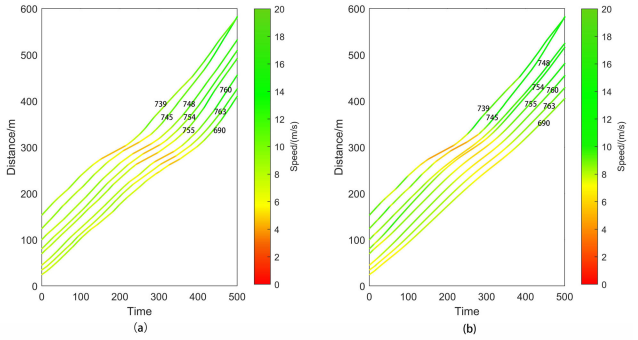

FIGURE 13. The time-space diagrams of the observed and simulated trajectory position with speeds in a platoon. (a) observed trajectory; (b) simulated trajectory.

VI. CONCLUSION

Data-driven car-following modeling is important for traffic simulation and the development of connected automated vehicle technology. This paper focuses on proposing an improved Seq2seq deep learning model (ISDL) for the CAVH environment. Firstly, the kinematics information of multiple preceding vehicles and host vehicles are extracted and organized into an input matrix according to the information topology of CAVs. Secondly, we proposed an improved Seq2seq framework that combines the Bi-GRU encoder, attention mechanism, and GRU decoder into an end-to-end fashion to learn the characteristics of the car-following behavior. Thirdly, the high-fidelity NGSIM data of car-following behavior with several preceding vehicles are employed to train, validate and test the ISDL model. Finally, the proposed model is compared with the IDM, the GRU, the LSTM, the SDL, and the GSDL model.

Several main findings are concluded from the experiments. (1) The simulated speeds and positions of the ISDL model are more accurate than those of the baseline models, indicating that the ISDL captures heterogeneous driving behaviors by mining the underlying information from the field data. (2) The introduction of multiple vehicle information is capable of improving the simulation performance of the deep learning-based car-following models in terms MAE_v, MAE_x, and MSE_x. (3) The proposed model can better reproduce the oscillating phenomenon between relative spacing and speed than the benchmark models. In addition, the ISDL model can provide the macroscopic stop-and-go waves in platoon simulation.

These findings shed light on the connected automated vehicle research area. One application is to generate neighboring human driving speed for CAV according to specific information flow topology. It can be employed to estimate the traffic condition through traffic oscillating simulation under the CAVH environment. Moreover, it can be expected that more vehicle dynamics parameters such as braking and steering, which are probably acquired through V2V communication in the practice of real-world CAVH environment, can be introduced as the input of the deep learning framework to predict the precise trajectory and motion of the vehicle.

REFERENCES

[1] R. Jiang, M.-B. Hu, H. M. Zhang, Z. Y. Gao, and Q.-S. Wu, "On some experimental features of car-following behavior and how to model them," *Transp. Res. B, Methodol.*, vol. 80, pp. 338–354, Oct. 2015.
[2] B. Ran, Y. Cheng, S. Li, F. Ding, J. Jin, X. Chen, and Z. Zhang, "Connected automated vehicle highway systems and methods," U.S. Patent, 2019.
[3] B. Ran, Y. Cheng, S. Li, Z. Zhang, F. Ding, H. Tan, Y. Wu, S. Dong, L. Ye, and X. Li, "Intelligent road infrastructure system (IRIS): Systems and methods," U.S. Patent, 2020.
[4] X. Chen, L. Li, and Y. Zhang, "A Markov model for headway/spacing distribution of road traffic," *IEEE Trans. Intell. Transp. Syst.*, vol. 11, no. 4, pp. 773–785, Dec. 2010.
[5] S. Ahn, M. J. Cassidy, and J. A. Laval, "Verification of a simplified car-following theory," *Transp. Res. B, Methodol.*, vol. 38, no. 5, pp. 431–440, 2004.
[6] J. Zhang, F.-Y. Wang, K. Wang, W.-H. Lin, X. Xu, and C. Chen, "Data-driven intelligent transportation systems: A survey," *IEEE Trans. Intell. Transp. Syst.*, vol. 12, no. 4, pp. 1624–1639, Dec. 2011.
[7] J. Morton, T. A. Wheeler, and M. J. Kochenderfer, "Analysis of recurrent neural networks for probabilistic modeling of driver behavior," *IEEE Trans. Intell. Transp. Syst.*, vol. 18, no. 5, pp. 1289–1298, May 2017.
[8] X. Wang, R. Jiang, L. Li, Y. Lin, X. Zheng, and F.-Y. Wang, "Capturing car-following behaviors by deep learning," *IEEE Trans. Intell. Transp. Syst.*, vol. 19, no. 3, pp. 910–920, Mar. 2018.
[9] X. Huang, J. Sun, and J. Sun, "A car-following model considering asymmetric driving behavior based on long short-term memory neural networks," *Transp. Res. C, Emerg. Technol.*, vol. 95, pp. 346–362, Oct. 2018.
[10] Y. Zheng, S. E. Li, J. Wang, L. Y. Wang, and K. Li, "Influence of information flow topology on closed-loop stability of vehicle platoon with rigid formation," in *Proc. 17th Int. IEEE Conf. Intell. Transp. Syst. (ITSC)*, Oct. 2014, pp. 2094–2100.
[11] V. Punzo, M. T. Borzacchiello, and B. Ciuffo, "On the assessment of vehicle trajectory data accuracy and application to the next generation simulation (NGSIM) program data," *Transp. Res. C, Emerg. Technol.*, vol. 19, pp. 1243–1262, Dec. 2011.
[12] Y. Li and D. Sun, "Microscopic car-following model for the traffic flow: The state of the art," *J. Control Theory Appl.*, vol. 10, no. 2, pp. 133–143, May 2012.
[13] P. G. Gipps, "A Behavioural car-following model for computer simulation," *Transp. Res. B, Methodol.*, vol. 15, no. 2, pp. 105–111, 1981.
[14] R. F. Benekohal and J. Treiterer, "CARSIM: Car-following model for simulation of traffic in normal and stop-and-go conditions," *Transp. Res. Rec.*, vol. 1194, pp. 99–111, Jan. 1988.
[15] W. van Winsum, "The human element in car following models," *Transp. Res. F, Traffic Psychol. Behav.*, vol. 2, no. 4, pp. 207–211, Dec. 1999.
[16] X. Zhao and Z. Gao, "A new car-following model: Full velocity and acceleration difference model," *Eur. Phys. J. B, Condens. Matter Complex Syst.*, vol. 47, pp. 145–150, Sep. 2005.
[17] G. H. Peng and D. H. Sun, "A dynamical model of car-following with the consideration of the multiple information of preceding cars," *Phys. Lett. A*, vol. 374, nos. 15–16, pp. 1694–1698, Apr. 2010.
[18] R. Jiang, Q. Wu, and Z. Zhu, "Full velocity difference model for a car-following theory," *Phys. Rev. E, Stat. Phys. Plasmas Fluids Relat. Interdiscip. Top.*, vol. 64, no. 1, p. 17101, Jun. 2001.
[19] D. C. Gazis, R. Herman, and R. W. Rothery, "Nonlinear follow-the-leader models of traffic flow," *Oper. Res.*, vol. 9, no. 4, p. 545–567, 1961.
[20] M. Treiber, A. Hennecke, and D. Helbing, "Congested traffic states in empirical observations and microscopic simulations," *Phys. Rev. E, Stat. Phys. Plasmas Fluids Relat. Interdiscip. Top.*, vol. 62, no. 2, pp. 1805–1824, Aug. 2000.
[21] Z.-W. Yi, W.-Q. Lu, L.-H. Xu, X. Qu, and B. Ran, "Intelligent back-looking distance driver model and stability analysis for connected and automated vehicles," *J. Central South Univ.*, vol. 27, no. 11, pp. 3499–3512, Nov. 2020.
[22] D. Wei and H. Liu, "Analysis of asymmetric driving behavior using a self-learning approach," *Transp. Res. B, Methodol.*, vol. 47, pp. 1–14, Jan. 2013.
[23] Z. He, L. Zheng, and W. Guan, "A simple nonparametric car-following model driven by field data," *Transp. Res. B, Methodol.*, vol. 80, pp. 185–201, Oct. 2015.
[24] J. Zheng, K. Suzuki, and M. Fujita, "Car-following behavior with instantaneous driver–vehicle reaction delay: A neural-network-based methodology," *Transp. Res. C, Emerg. Technol.*, vol. 36, pp. 339–351, Nov. 2013.
[25] A. Khodayari, A. Ghaffari, R. Kazemi, and R. Braunstingl, "A modified car-following model based on a neural network model of the human driver effects," *IEEE Trans. Syst., Man, Cybern. A, Syst. Humans*, vol. 42, no. 6, pp. 1440–1449, Nov. 2012.
[26] J. Hongfei, J. Zhicai, and N. Anning, "Develop a car-following model using data collected by 'five-wheel system,'" in *Proc. IEEE Int. Conf. Intell. Transp. Syst.*, Oct. 2003, pp. 346–351.
[27] S. Panwai and H. Dia, "Neural agent car-following models," *IEEE Trans. Intell. Transp. Syst.*, vol. 8, no. 1, pp. 60–70, Mar. 2007.
[28] H. Jiang, L. Chang, Q. Li, and D. Chen, "Trajectory prediction of vehicles based on deep learning," in *Proc. 4th Int. Conf. Intell. Transp. Eng. (ICITE)*, Sep. 2019, pp. 190–195.
[29] Z. Mofan, Q. Xiaobo, and L. Xiaopeng, "A recurrent neural network based microscopic car following model to predict traffic oscillation," *Transport. Res. C, Emerg. Technol.*, vol. 84, pp. 245–264, Nov. 2017.
[30] Y. Lin, P. Wang, Y. Zhou, F. Ding, C. Wang, and H. Tan, "Platoon trajectories generation: A unidirectional interconnected LSTM-based car-following model," *IEEE Trans. Intell. Transp. Syst.*, vol. 23, no. 3, pp. 2071–2081, Mar. 2022.
[31] Z. Hao, X. Huang, K. Wang, M. Cui, and Y. Tian, "Attention-based GRU for driver intention recognition and vehicle trajectory prediction," in *Proc. 4th CAA Int. Conf. Veh. Control Intell. (CVCI)*, Dec. 2020, pp. 86–91.
[32] I. Sutskever, O. Vinyals, and Q. V. Le, "Sequence to sequence learning with neural networks," in *Proc. Adv. Neural Inf. Process. Syst.*, 2014, pp. 3104–3112.
[33] K. Sun, T. Qian, X. Chen, and M. Zhong, "Context-aware Seq2Seq translation model for sequential recommendation," *Inf. Sci.*, vol. 581, pp. 60–72, Dec. 2021.
[34] Y. Zhang and W. Xiao, "Keyphrase generation based on deep Seq2Seq model," *IEEE Access*, vol. 6, pp. 46047–46057, 2018.
[35] L. You, S. Xiao, Q. Peng, C. Claramunt, X. Han, Z. Guan, and J. Zhang, "ST-Seq2Seq: A spatio-temporal feature-optimized Seq2Seq model for short-term vessel trajectory prediction," *IEEE Access*, vol. 8, pp. 218565–218574, 2020.
[36] R. Das, R. Bo, H. Chen, W. Ur Rehman, and D. Wunsch, "Forecasting nodal price difference between day-ahead and real-time electricity markets using long-short term memory and sequence-to-sequence networks," *IEEE Access*, vol. 10, pp. 832–843, 2022.

[37] K. Cho, B. van Merrienboer, C. Gulcehre, D. Bahdanau, F. Bougares, H. Schwenk, and Y. Bengio, "Learning phrase representations using RNN encoder–decoder for statistical machine translation," 2014, *arXiv:1406.1078*.
[38] L. Li, J. Zhang, Y. Wang, and B. Ran, "Missing value imputation for traffic-related time series data based on a multi-view learning method," *IEEE Trans. Intell. Transp. Syst.*, vol. 20, no. 8, pp. 2933–2943, Aug. 2018.
[39] K. Palasundram, N. Mohd Sharef, K. A. Kasmiran, and A. Azman, "SEQ2SEQ++: A multitasking-based Seq2Seq model to generate meaningful and relevant answers," *IEEE Access*, vol. 9, pp. 164949–164975, 2021.
[40] X. Zhao, Y. Shao, J. Mai, A. Yin, and S. Xu, "Respiratory sound classification based on BiGRU-attention network with XGBoost," in *Proc. IEEE Int. Conf. Bioinf. Biomed. (BIBM)*, Dec. 2020, pp. 915–920.
[41] W. Lu, Z. Yi, R. Wu, Y. Rui, and B. Ran, "Traffic speed forecasting for urban roads: A deep ensemble neural network model," *Phys. A, Stat. Mech. Appl.*, vol. 593, May 2022, Art. no. 126988.
[42] Z. Yi, W. Lu, X. Qu, J. Gan, L. Li, and B. Ran, "A bidirectional car-following model considering distance balance between adjacent vehicles," *Phys. A, Stat. Mech. Appl.*, vol. 603, Oct. 2022, Art. no. 127606.
[43] A. Kesting and M. Treiber, "Calibrating car-following models by using trajectory data: Methodological study," *Transp. Res. Rec., J. Transp. Res. Board*, vol. 2088, no. 1, pp. 148–156, 2008.
[44] B. Coifman and L. Li, "A critical evaluation of the next generation simulation (NGSIM) vehicle trajectory dataset," *Transp. Res. B, Methodol.*, vol. 105, pp. 362–377, Nov. 2017.
[45] S. Hochreiter and J. Schmidhuber, "Long short-term memory," *Neural Comput.*, vol. 9, no. 8, pp. 1735–1780, 1997.
[46] L. Ma and S. Qu, "A sequence to sequence learning based car-following model for multi-step predictions considering reaction delay," *Transp. Res. C, Emerg. Technol.*, vol. 120, Nov. 2020, Art. no. 102785.
[47] M. Green, "'How long does it take to stop?' methodological analysis of driver perception-brake times," *Transp. Hum. Factors*, vol. 2, no. 3, pp. 195–216, 2000.
[48] V. Papathanasopoulou and C. Antoniou, "Towards data-driven car-following models," *Transp. Res. C, Emerg. Technol.*, vol. 55, pp. 496–509, Jun. 2015.
[49] J. Xie and M. Zhu, "Maneuver-based driving behavior classification based on random forest," *IEEE Sensors Lett.*, vol. 3, no. 11, pp. 1–4, Nov. 2019.
[50] M. Saifuzzaman and Z. Zheng, "Incorporating human-factors in car-following models: A review of recent developments and research needs," *Transp. Res. C, Emerg. Technol.*, vol. 48, pp. 379–403, Nov. 2014.

WENQI LU received the B.E. degree in transportation engineering from Hohai University, Nanjing, China, in 2016, and the M.S. degree in transportation planning and management from Beijing Jiaotong University, Beijing, China, in 2019. He is currently pursuing the Ph.D. degree with the School of Transportation, Southeast University, Nanjing. His current research interests include connected and automated vehicles, traffic theory, and intelligent transportation systems.

ZIWEI YI received the B.E. degree in transportation engineering from the Harbin Institute of Technology, Harbin, China, in 2017. She is currently pursuing the Ph.D. degree with the School of Transportation, Southeast University, Nanjing, China. Her research interests include traffic flow theory and intelligent vehicles.

BINGJIE LIANG received the B.E. degree in transportation from Dalian Maritime University. He is currently pursuing the Ph.D. degree with the School of Traffic and Transportation, Beijing Jiaotong University. His research interests include intelligent transportation systems, information technology, and the applications of the operational research in the field of transportation.

YIKANG RUI received the Ph.D. degree in geographic information science from the KTH Royal Institute of Technology. He was a Postdoctoral Fellow with Nanjing University, from 2014 to 2016. He is currently an Associate Research Fellow with the School of Transportation, Southeast University, Nanjing, China. His current research interests include spatio-temporal data model, traffic network analysis, and vehicle-road collaborative decision planning.

BIN RAN is currently the Director of the Joint Research Institute on Internet of Mobility, founded by Southeast University, China, and the University of Wisconsin–Madison, Madison, WI, USA. He also holds the title of the National Distinguished Expert in China and the Vilas Distinguished Achievement Professor and the Director of the Intelligent Transportation System (ITS) Program with the University of Wisconsin–Madison. He mainly engages in the research studies of intelligent transportation systems and connected automated vehicle highway (CAVH) systems. He is the founding President of the Chinese Overseas Transportation Association (COTA). He is also an Associate Editor of the *Journal of Intelligent Transportation Systems*.